Thermochimica Acta, 33 (1979) 51—67

THERMOANALYTICAL STUDY ON THE OXIDATION OF URANIUM DIOXIDES DERIVED FROM URANYL NITRATE, URANYL ACETATE AND AMMONIUM DIURANATE

RYUSABURO FURUICHI, TADAO ISHII and TOSHIAKI NAKANE

Department of Applied Chemistry, Faculty of Engineering, Hokkaido University, Sapporo 060 (Japan)

(Received 27 October 1978)

ABSTRACT

The oxidation of UO_2 was investigated by TG, DSC and X-ray diffraction. UO_2 samples were prepared by the reduction of UO_3 at $P_{H_2} + P_{N_2} = 100 + 50$ mm Hg and 5°C min^{-1} up to 800°C. In order to obtain six UO_2 samples with different preparative histories, UNH, UAH and ADU were used as starting materials and their thermal decomposition was carried out at 450—625°C for 0—9 h at an air flow rate of 100 ml min^{-1}. α-UO_3, γ-UO_3, $UO_3 \cdot 2\,H_2O$, and their mixtures were obtained. The reduction of UO_3 gave β-UO_{2+x} with different x values from 0.030 to 0.055. The oxidation carried out at P_{O_2} = 150 mm Hg was found to consist of oxygen uptake at room temperature, $UO_2 \rightarrow U_3O_7$ (Step I) and $U_3O_7 \rightarrow U_3O_8$ (Step II). TG and DSC curves of the oxidation showed two plateaus and two exothermic peaks corresponding to Steps I and II. In the case of two of the samples, the DSC peak of Step II split into two substeps, which were assumed to be due to the different reactivities of U_3O_7 formed from α-UO_3 and that from other types of UO_3. The increase in O/U ratio due to the oxygen uptake at room temperature changed from 0.010 to 0.042 except for a sample prepared from ADU which showed an extraordinarily large value of 0.445. TG curves showed an increase in O/U from room temperature to near 250°C for Step I and the plateau at 250—350°C where O/U was about 2.42, and showed a sharp increase in O/U above 350°C for Step II and the plateau above 400°C where O/U was 2.72—2.75. It is thought that the prepared UO_2 had a defective structure with a large interstitial volume to accommodate the excess oxygen.

INTRODUCTION

The oxidation reaction of uranium dioxide (UO_2) has been extensively investigated in order to understand the oxidation mechanism of the non-stoichiometric oxide and for purposes of reactor safety [1—12]. It is generally accepted that the oxidation process at temperatures above 250°C proceeds via two successive steps from UO_2 to U_3O_7 (Step I) and from U_3O_7 to U_3O_8 (Step II), and that Step I is controlled by the rate of diffusion of oxygen through the UO_2 lattice or product layer and Step II is controlled by the rate of nucleation and/or the growth rate. On the other hand, the reactivity of UO_2 powder, such as its solubility in acids, sinterability and oxidation rate or temperature, has been observed to change remarkably with a slight difference in preparation history of the oxide [3,13—15]. This leads to difficulty in obtaining reproducible results for the oxide preparation.

Accordingly, it is necessary to elucidate the relation between the reactivity of the oxide and its preparation history. In previous experiments, many authors used isothermal techniques and the kinetic method. The present authors showed in studies on ferric oxide, aluminium oxides and chromic oxide that the non-isothermal techniques such as DTA and TG were also very useful and convenient for investigating the reactivity of oxides [16—20]. In the present paper, the results of oxidation experiments are described for six UO_2 samples prepared under different conditions and for commercial UO_2. Samples of uranium trioxide (UO_3) were used as the precursor of UO_2. These were obtained by the thermal decomposition of uranium nitrate hydrate (UNH), uranium acetate hydrate (UAH) and ammonium diuranate (ADU). The reduction of UO_3 by H_2 and the oxidation of the resultant UO_2 by O_2 were examined by use of TG, DSC and X-ray techniques.

EXPERIMENTAL

Materials

UNH ($UO_2(NO_3)_2 \cdot 6\,H_2O$) and UAH ($UO_2(CH_3COO)_2 \cdot 2\,H_2O$) were GR grade reagents from Nakarai Chem. Co. A UO_2 powdered sample was obtained commercially from Mitsubishi Metal Co. ADU [$(NH_4)_2U_2O_7$] [21] was prepared by adding NH_4OH solution to a solution of UNH (100 g H_2O + 50 g UNH) until a pH of 10.6 was reached. The orange precipitate was stood for 2 h at 50—90°C in the mother liquor and then washed well with water. The sample dried at 100°C for 3 h showed an X-ray pattern in agreement with ASTM 13-59. H_2, O_2 and N_2 were all cylinder gases.

TG

The apparatus was a Cahn electrobalance Model RG with a quartz hang-down tube (d = 35 mm). The sample was placed in a quartz basket (10 × 10 mm) suspended from the arm of balance by means of a quartz wire (0.3 mm). The sample temperature was measured with a chromel—alumel thermocouple by putting its tip at 5 mm below the bottom of basket. The atmospheres used were static, P_{O_2} = 150 mm Hg and $P_{H_2} + P_{N_2}$ = 100 + 50 mm Hg At a pressure of 150 mm Hg, the buoyancy effect was observed to be constant up to 1000°C. The heating rate was fixed by an ECP-51B type program controller (Ohkura Electronics Ins.).

DSC

A thermoflex type 8001 (Rigaku Denki) was used in conjunction with platinum holders (5 × 2 mm) and a 10—20 mg sample. The measurements were carried out with α-Al_2O_3 (Merck) as reference material in static air.

X-Ray diffraction

A geigerflex type 2004 diffractometer (Rigaku Denki) was operated under the conditions of Co-target, Fe-filter, 35 kV and 10 mA.

Decomposition of UNH, UAH and ADU

Isothermal decomposition was carried out to obtain UO_3 at programmed temperatures in an air flow (100 ml min^{-1}) by using a tube furnace and an alumina boat.

Estimation of the O/U ratio

On the basis of the results of Biltz and Muller [22] that the stoichiometric U_3O_8 was stable in air at 700—720°C, the O/U ratio was estimated from the weight of sample measured after it was oxidized to U_3O_8 at P_{O_2} = 150 mm Hg and 720°C.

RESULTS AND DISCUSSION

Thermal decomposition of UNH, UAH and ADU

In order to fix the preparation conditions of UO_3, TG experiments on the decomposition of these three uranium salts were carried out in an O_2 atmosphere (P_{O_2} = 150 mm Hg). The results are shown in Fig. 1 where ΔW_t is the weight decrease at temperature t°C and ΔW_T is the total weight decrease. TG curves indicate that the main weight decrease finishes below 400°C and the minor weight decrease occurs at about 600°C for UNH and ADU. X-ray results revealed that the decomposition products of the three salts removed at 720°C were all U_3O_8 (ASTM 2-0276). It has been reported that UO_3 is formed by the isothermal calcination of UNH and ADU in air at 500°C [14,23] and is decomposed to U_3O_8 at 600°C [24]. The small weight

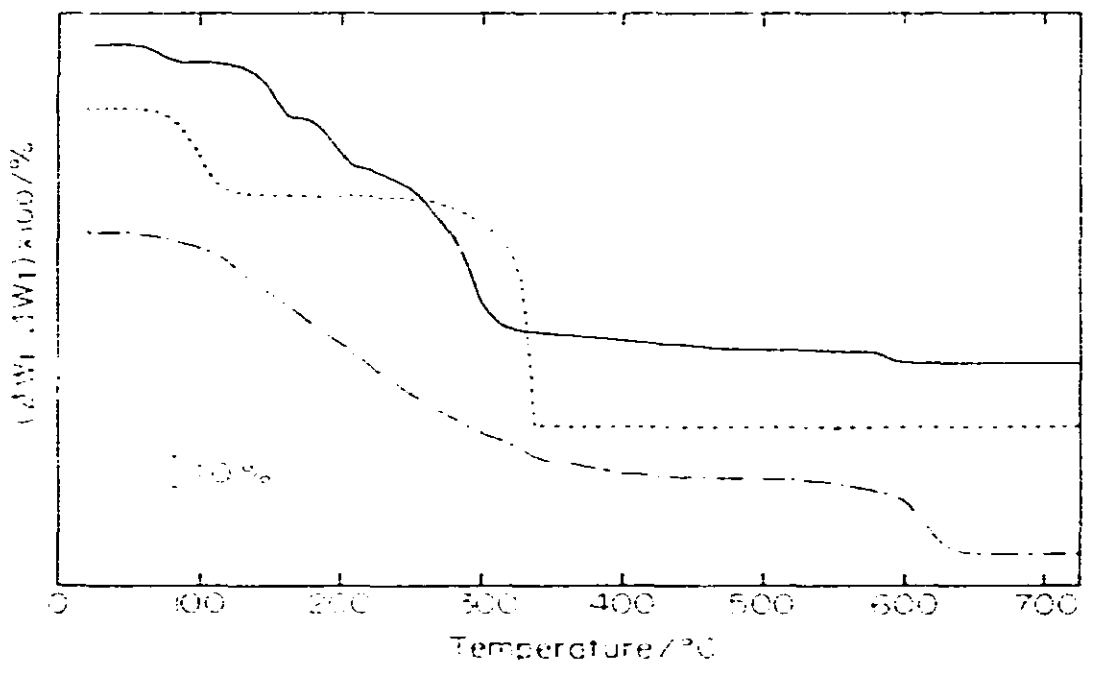

Fig. 1. TG curves of thermal decomposition of UNH (———, sample weight = 38.2 mg), UAH (- - - - - -, 13.5 mg) and ADU (· — · — ·, 38.96 mg) in oxygen. P_{O_2} = 150 mm Hg, heating rate = 5°C min^{-1}, ΔW_t = wt. decrease at temperature t°C, ΔW_T = total wt. decrease.

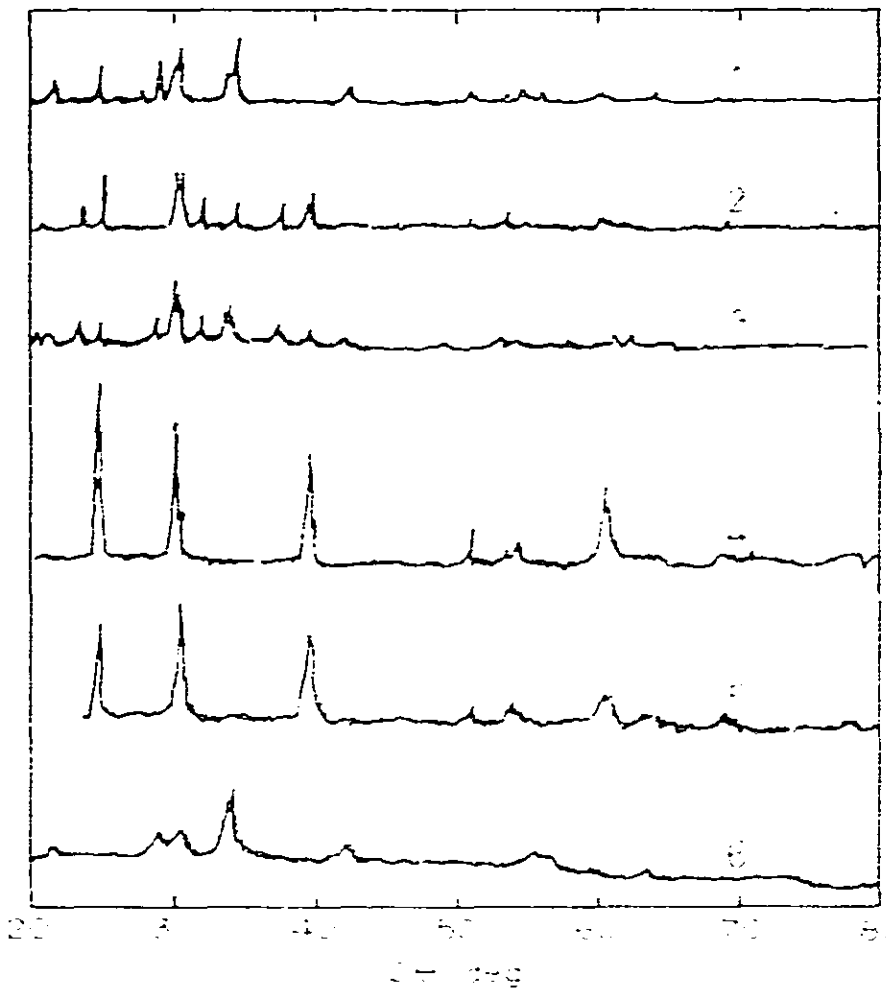

Fig. 2. X-Ray diffraction patterns of UO_3 samples. 1, UO_3(50-8); 2, UO_3(50-9); 3, UO_3 (52-4); 4, UO_3(62-0); 5, UO_3(45-5); 6, UO_3(50-1). Preparative conditions are shown in Table 1.

decrease observed near 600°C in Fig. 1 is considered to correspond to the formation of U_3O_8 from UO_3. In the case of UAH, however, there is no weight change above 340°C. This fact may indicate that the decomposition of UAH to form U_3O_8 was completed at 340°C and was accompanied by the reduction of the U^{n+} ion by the CO formed from the acetate ion. A similar reduction was observed in the formation of Fe_3O_4 from ferric acetate [18]. Figure 1 shows that UO_3 can be obtained by thermal decomposition at tem-

TABLE 1

Decomposition conditions of uranium salts for the preparation of UO_3 samples

Salt	Decomposition		Atmosphere	UO_3 formed	Symbol
	Temp. (°C)	Time (h)			
UNH [a]	500	8	air flow	γ-UO_3, $UO_3 \cdot 2\,H_2O$	UO_3 (50-8)
UNH	500	9	(100 ml min^{-1})	α-UO_3, γ-UO_3	UO_3 (50-9)
UNH	525	4		γ-UO_3, $UO_3 \cdot 2\,H_2O$	UO_3 (52-4)
UNH	625	0 [d]		α-UO_3, U_3O_8	UO_3 (62-0)
UAH [b]	450	5		α-UO_3	UO_3 (45-5)
ADU [c]	505	1		$UO_3 \cdot 2\,H_2O$	UO_3 (50-1)

[a] Uranyl nitrate hydrate.
[b] Uranyl acetate hydrate.
[c] Ammonium diuranate.
[d] Heated up to 625°C at a rate of 10°C min^{-1}.

peratures between 400 and 600°C. In order to obtain a sufficient amount of UO_3 sample for the experiments, the uranium salt (4—5 g) was isothermally calcined in an alumina boat at an air flow rate of 100 ml min^{-1} at various temperatures for various periods of time. Six UO_3 samples were prepared and

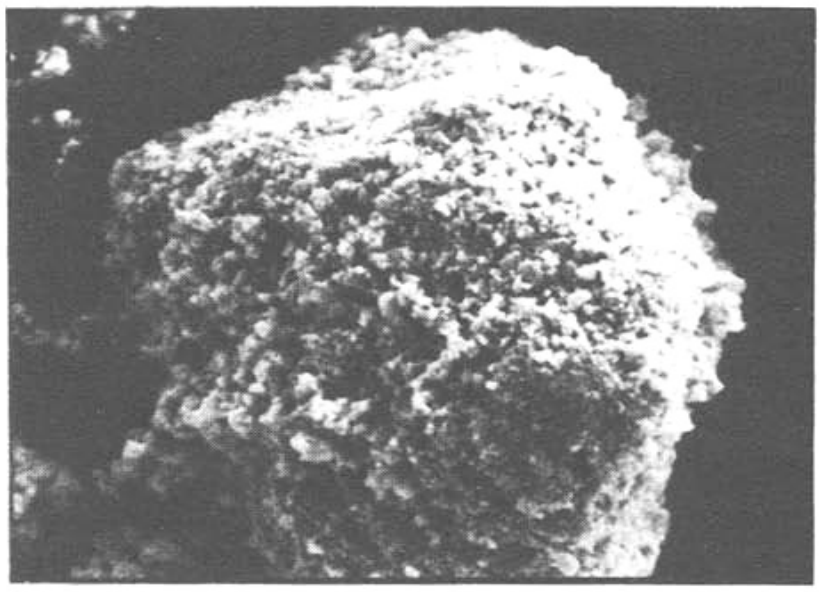

(a) UO_3(50-8)

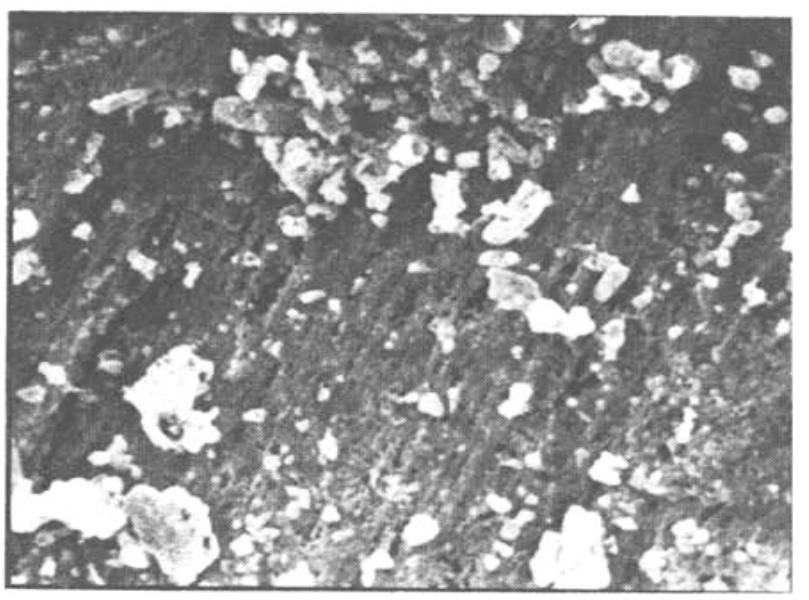

(d) UO_3(45-5)

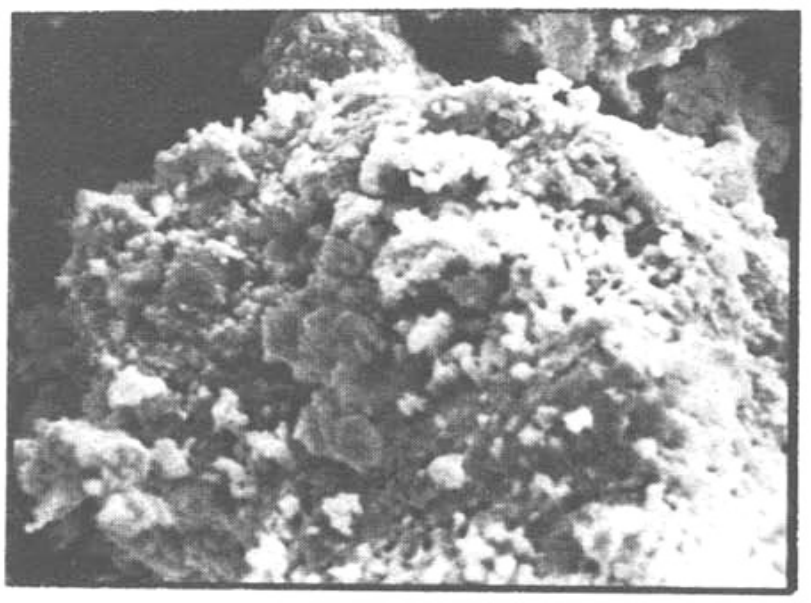

(b) UO_3(50-9)

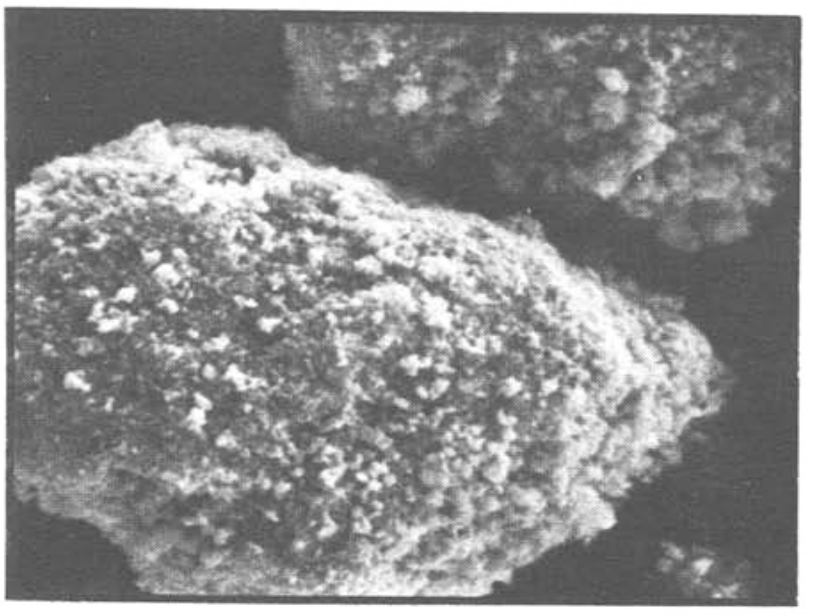

(e) UO_3(50-1)

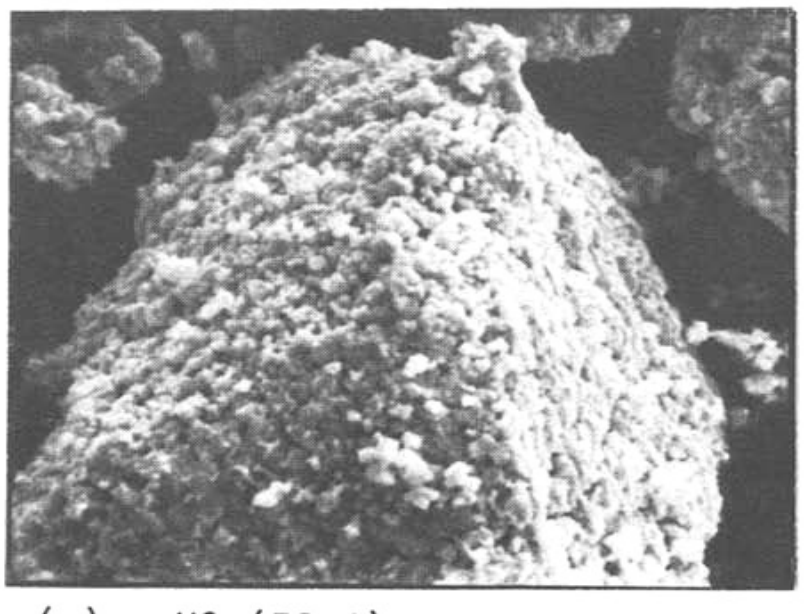

(c) UO_3(52-4)

2 μm

Fig. 3. Scanning electron micrographs of UO_3 samples.

their X-ray patterns and SEM photographs are shown in Figs. 2 and 3. Table 1 contains the preparation conditions, UO_3 phases identified by X-ray results in Fig. 2 and symbols for distinguishing between the samples. It is found that the α-UO_3 phase is formed when the decomposition is carried out at higher temperatures for longer periods of time. None of the UO_3 prepared from UNH indicated IR absorption bands due to the remaining NO_3^- ion.

Reduction of UO_3 to UO_2

The reduction was carried out using TG apparatus and 60—70 mg of UO_3 at $P_{H_2} + P_{N_2} = 100 + 50$ mm Hg. Figure 4 shows the results for six UO_3 and for commerical UO_2 [UO_2(C)]. O/U ratios at room temperature are 3.219, 3.189, 3.167 and 3.095 (>3) for UO_3(50-9), (52-4), (50-1) and (50-8), 3.005 (≃3) for UO_3(45-5) and 2.852 (<3) for UO_3(62-0), respectively. As shown in Fig. 2 and Table 1, UO_3(45-5) is a single phase of α-UO_3 (O/U = 3) and UO_3(62-0) is a mixture of α-UO_3 and U_3O_8 (O/U < 3). UO_3 samples of O/U > 3 contain γ-UO_3 and/or $UO_3 \cdot 2\,H_2O$, and show the broad X-ray patterns indicating low crystallinity. It is considered that the hydrated water leads to a larger O/U than 3. The amount of water was calculated by assuming a reaction, $UO_3 \cdot n\,H_2O + (1-x)\,H_2 = UO_{2+x} + (1-x)\,H_2O + n\,H_2O$. The values of $(2+x)$ were estimated from O/U values at 800°C in Fig. 4. They are shown in Table 2. The amounts of hydrated water estimated are n = 0.193, 0.168, 0.148 and 0.083 for UO_3(50-9), (52-4), (50-1) and (50-8).

It is observed in Fig. 4 that the TG results for UO_3(50-1), curve 3, show a break around O/U = 2.58 and the reduction proceeds at temperatures about

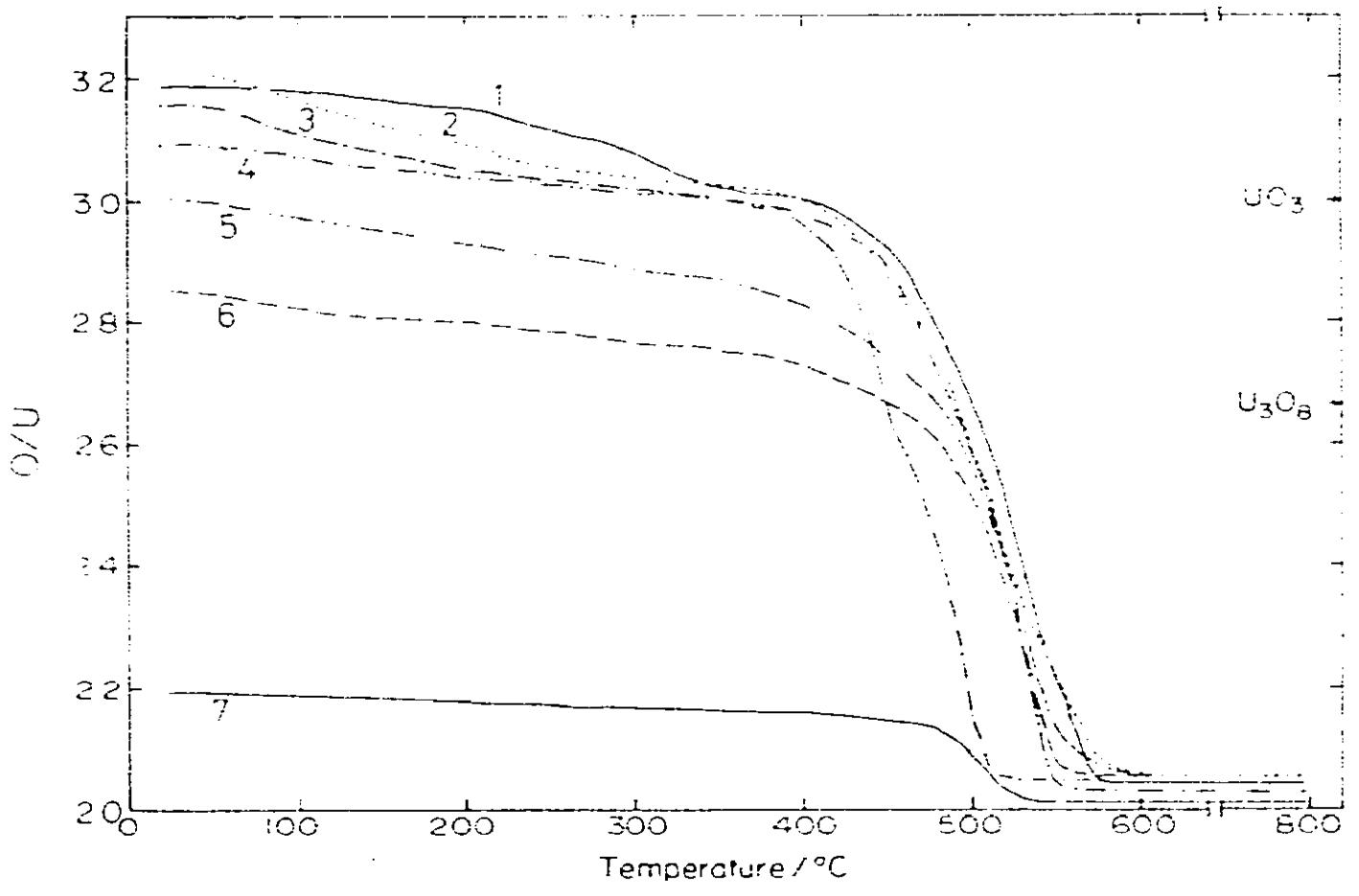

Fig. 4. TG curves of reduction of UO_3 samples and commercial UO_2. 1, UO_3(52-4); 2, UO_3(50-9); 3, UO_3(50-1); 4, UO_3(50-8); 5, UO_3(45-5); 6, UO_3(62-0); 7, commercial UO_2 (UO_2(C)). $P_{H_2} + P_{N_2}$ = 100 + 50 mm Hg, heating rate = 5° min^{-1}.

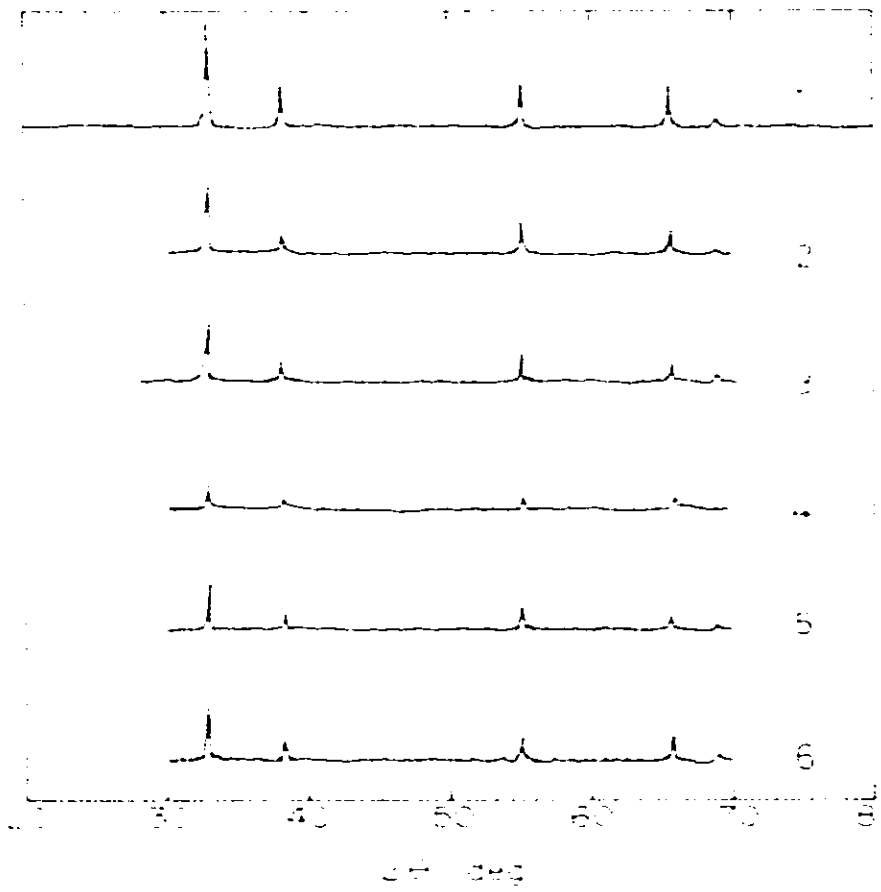

Fig. 5. X-Ray diffraction patterns of UO_2 obtained by reduction of UO_3 up to 800°C. 1, Commercial UO_2; 2, UO_2(50-8); 3, UO_2(50-9); 4, UO_2(52-4); 5, UO_2(45-5); 6, UO_2 (62-0).

50°C lower than other UO_3 samples. DeMarco et al. [25] and LePage et al. [26] observed the change in reduction rate and the formation of U_3O_8 near O/U = 2.6 in the isothermal experiments. They concluded that the reduction of UO_3 proceeded consecutively via two steps; the first is UO_3 to U_3O_8 and the second is U_3O_8 to UO_2. The break in the TG curve in Fig. 4 may be explained as follows; UO_3(50-1), which was obtained from ADU, has a high reactivity compared with other UO_3 samples, therefore the first reduction step proceeds at lower temperatures and its rate is higher than that of the second step. The difference between the rates of the first and the second step may result in the break in the TG curve. UO_3(50-8) shows a very slight break near O/U = 2.67.

Figure 5 shows the X-ray patterns of UO_2 samples which were taken out

TABLE 2

UO_2 samples prepared by reduction of UO_3

Starting UO_3	Composition of UO_2 formed	Crystallite size (Å)	Symbol for UO_2 sample
UO_3 (50-8)	$UO_{2.030}$	530—620	UO_2 (50-8)
UO_3 (50-9)	$UO_{2.055}$	520—680	UO_2 (50-9)
UO_3 (52-4)	$UO_{2.041}$	450—620	UO_2 (52-4)
UO_3 (62-0)	$UO_{2.049}$	350—620	UO_2 (62-0)
UO_3 (45-5)	$UO_{2.044}$	550—760	UO_2 (45-5)
UO_3 (50-1)	$UO_{2.039}$		UO_2 (50-1)
Commercial UO_2	$UO_{2.007}$	1280—1730	UO_2 (C)

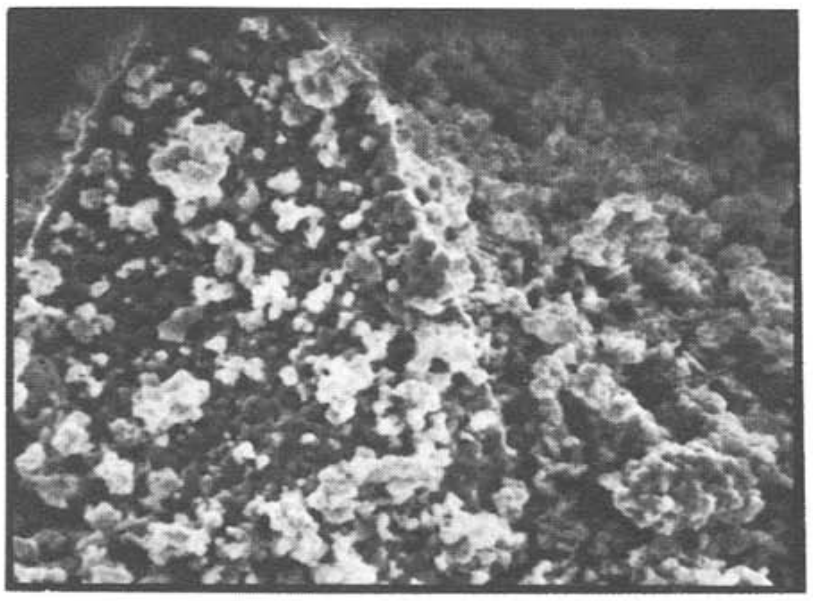

(a) UO_2(C)

(d) UO_2(52-4)

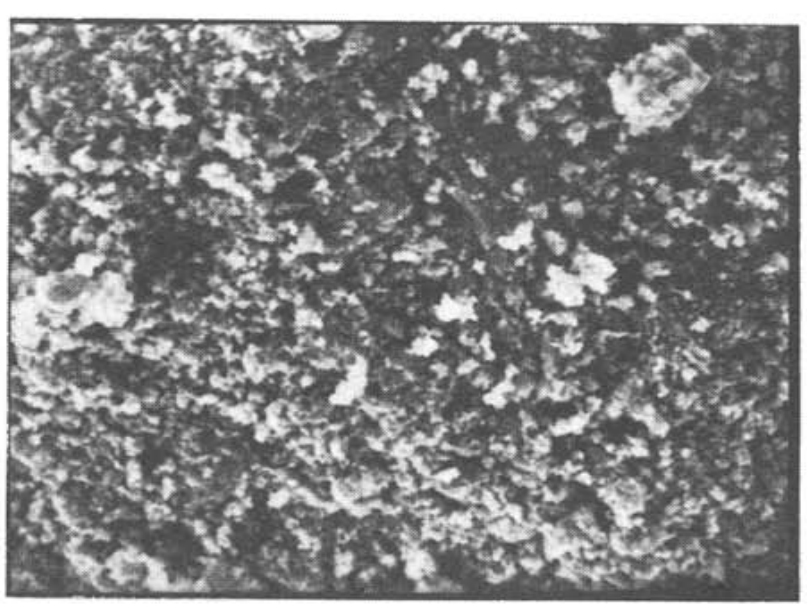

(b) UO_2(50-8)

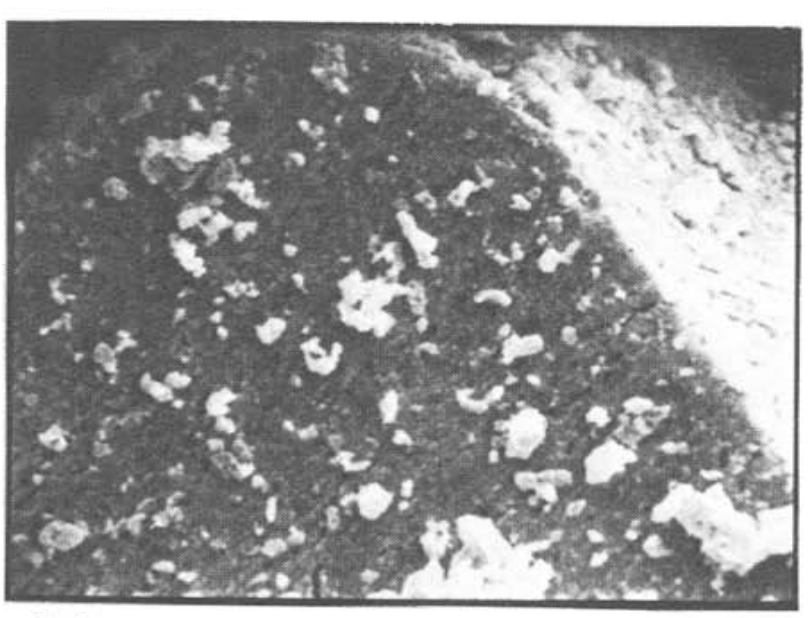

(e) UO_2(45-5)

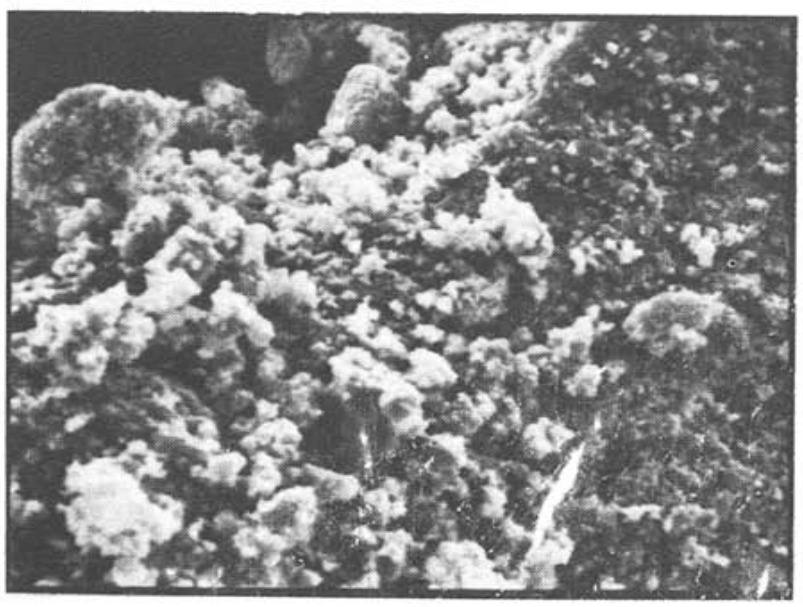

(c) UO_2(50-9)

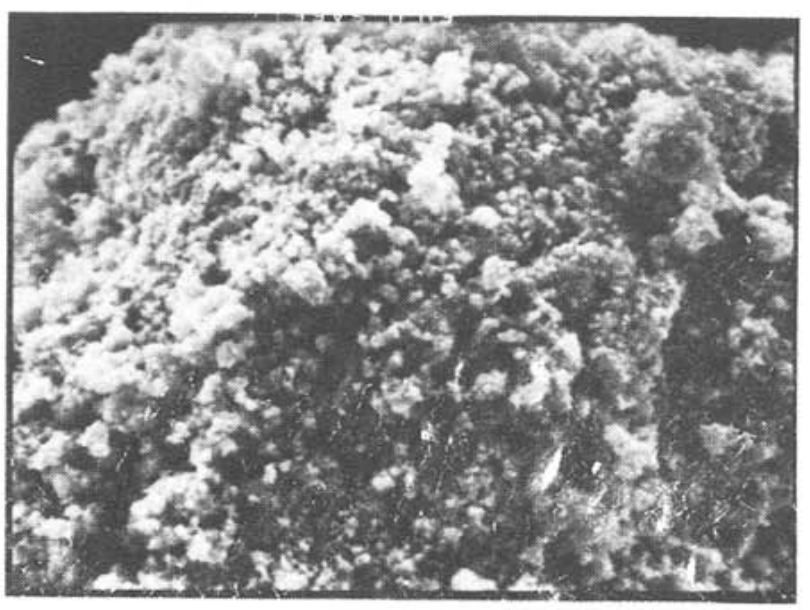

(f) UO_2(50-1)

2 μm

Fig. 6. Scanning electron micrographs of UO_2 samples.

of the apparatus after cooling from 800°C to room temperature in H_2. Figure 6 shows their SEM photographs. From X-ray results, all UO_2 samples are identified as β-UO_2 (ASTM 9-206) and the order of intensity of X-ray diffraction lines is UO_2(C) >> UO_2(50-8) > (50-9) ≃ (45-5) ≃ (62-0) > (52-4). The crystallite size (d) was calculated from the line widths at 2θ = 32.9, 38.2 and 55.1° (Table 2). It is found from Table 2 that the commercial UO_2 shows the largest d and the preparation conditions do not affect the d value of UO_2, but result in different amounts of excess oxygen in the UO_2 formed.

Oxidation of UO_2 to U_3O_8

As mentioned in the preceeding section, UO_2 samples were obtained by the reduction of UO_3 at 5° min^{-1} up to 800°C at $P_{H_2} + P_{N_2}$ = 100 + 50 mm Hg in the TG equipment. For the TG experiments on the oxidation, O_2 (P_{O_2} = 150 mm Hg) was introduced into the TG apparatus after the UO_2 formed had been cooled in H_2 from 800°C to room temperature and then evacuated for 3 h. For the DSC experiments, the cooled UO_2 was taken out of the apparatus and placed in the sample holder to weigh in air. Figures 7--10 are the results for TG and DSC for the oxidation. In Fig. 10, the solid curve is the result of the first oxidation of fresh UO_2 formed from UO_3(50-1) and the dotted curve is that of the re-oxidation of UO_2 which was obtained

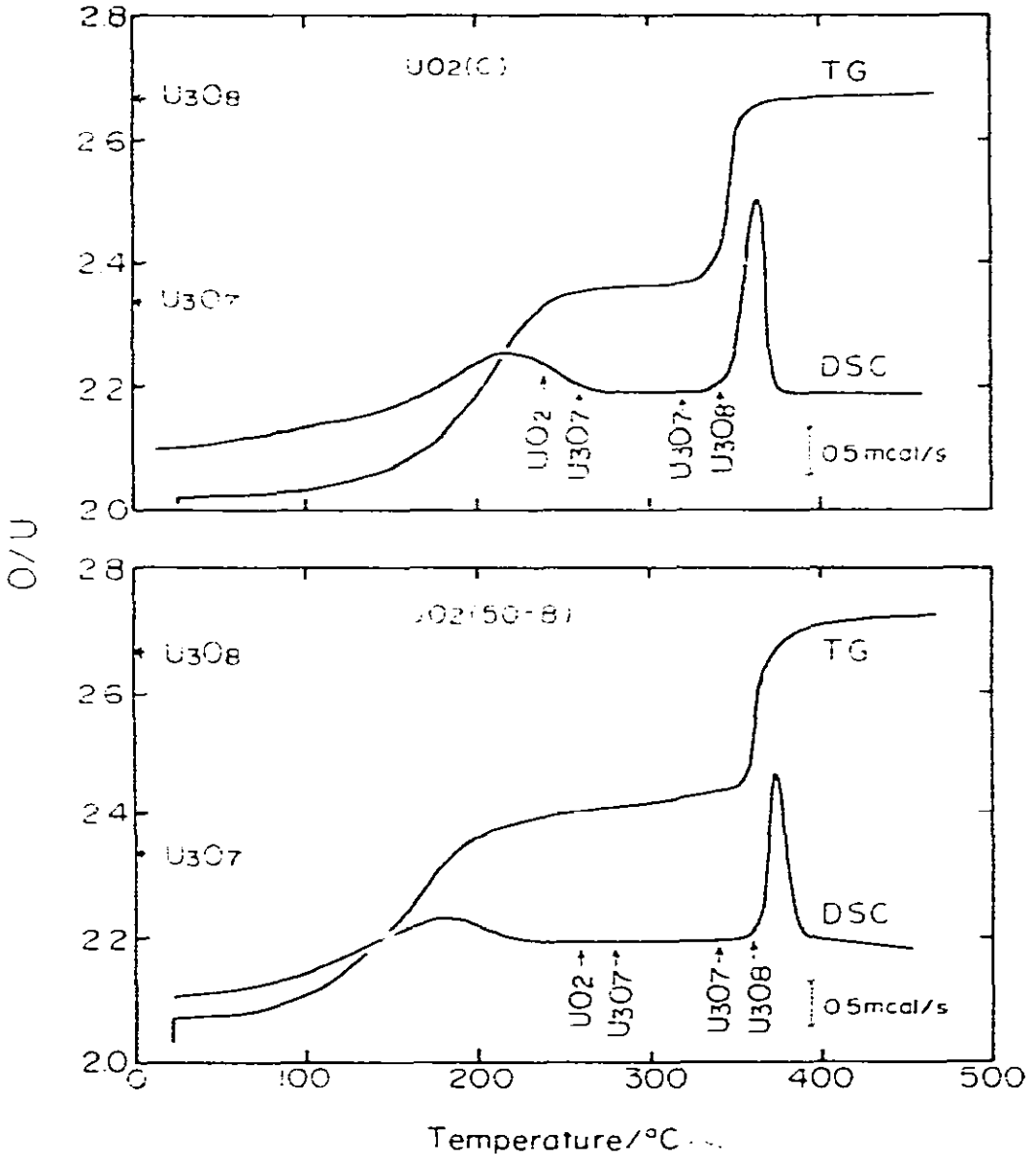

Fig. 7. TG and DSC curves of oxidation of UO_2(C) and UO_2(50-8). TG: 5°C min^{-1}, P_{O_2} = 150 mm Hg; DSC: 10°C min^{-1}, air.

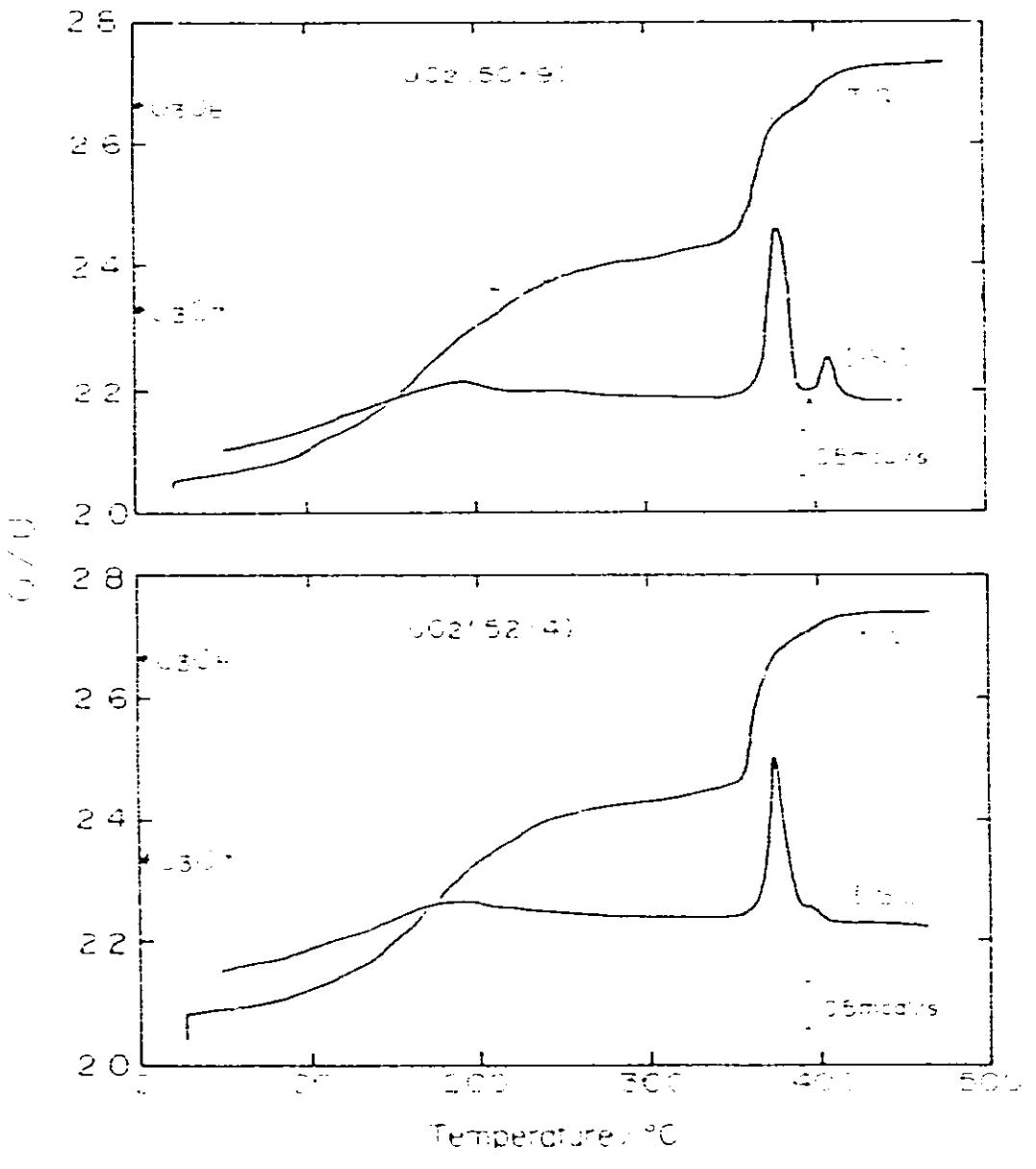

Fig. 8. TG and SDC curves of oxidation of UO_2(50-9) and UO_2(52-4).

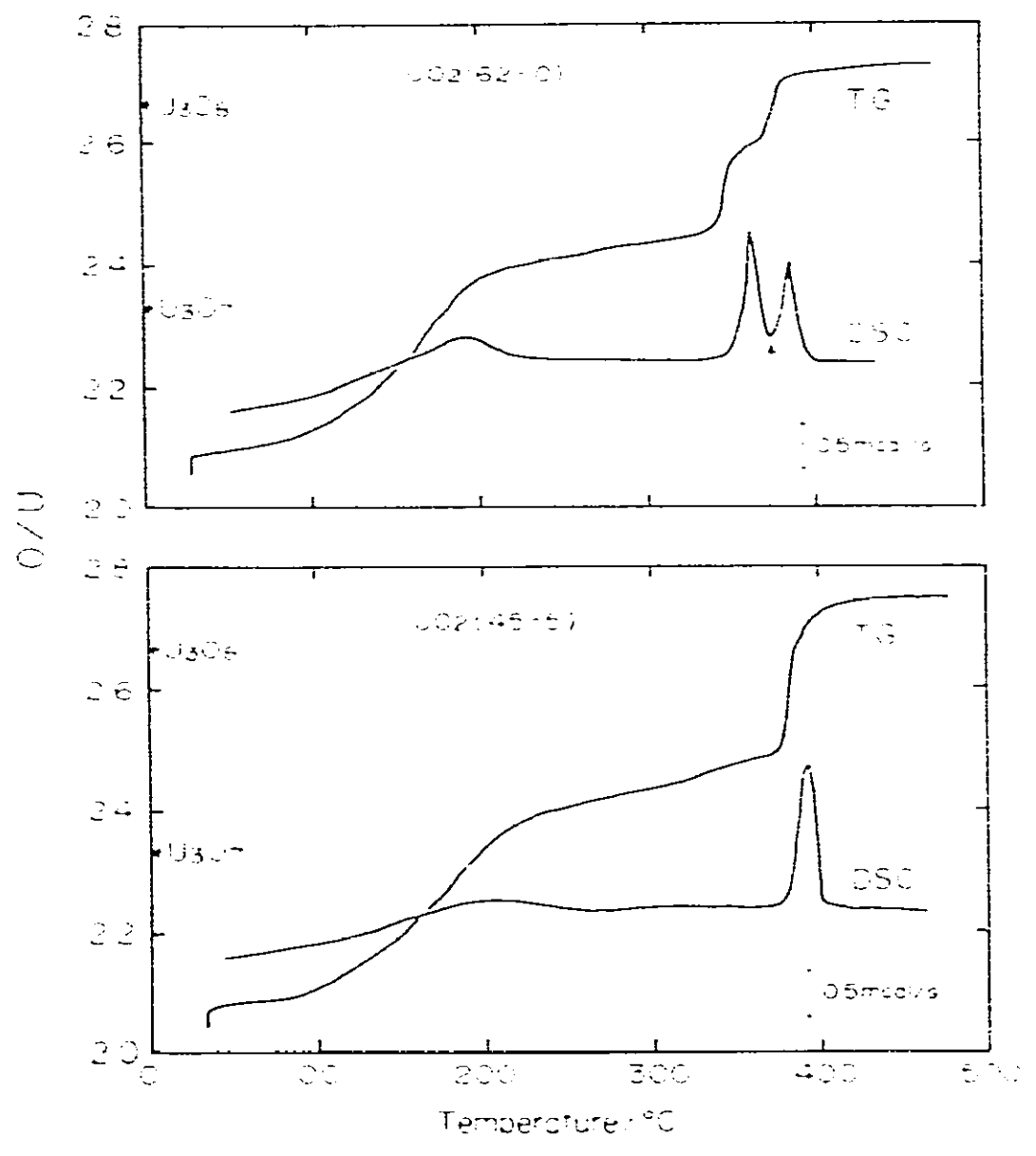

Fig. 9. TG and DSC curves of oxidation of UO_2(62-0) and UO_2(45-5).

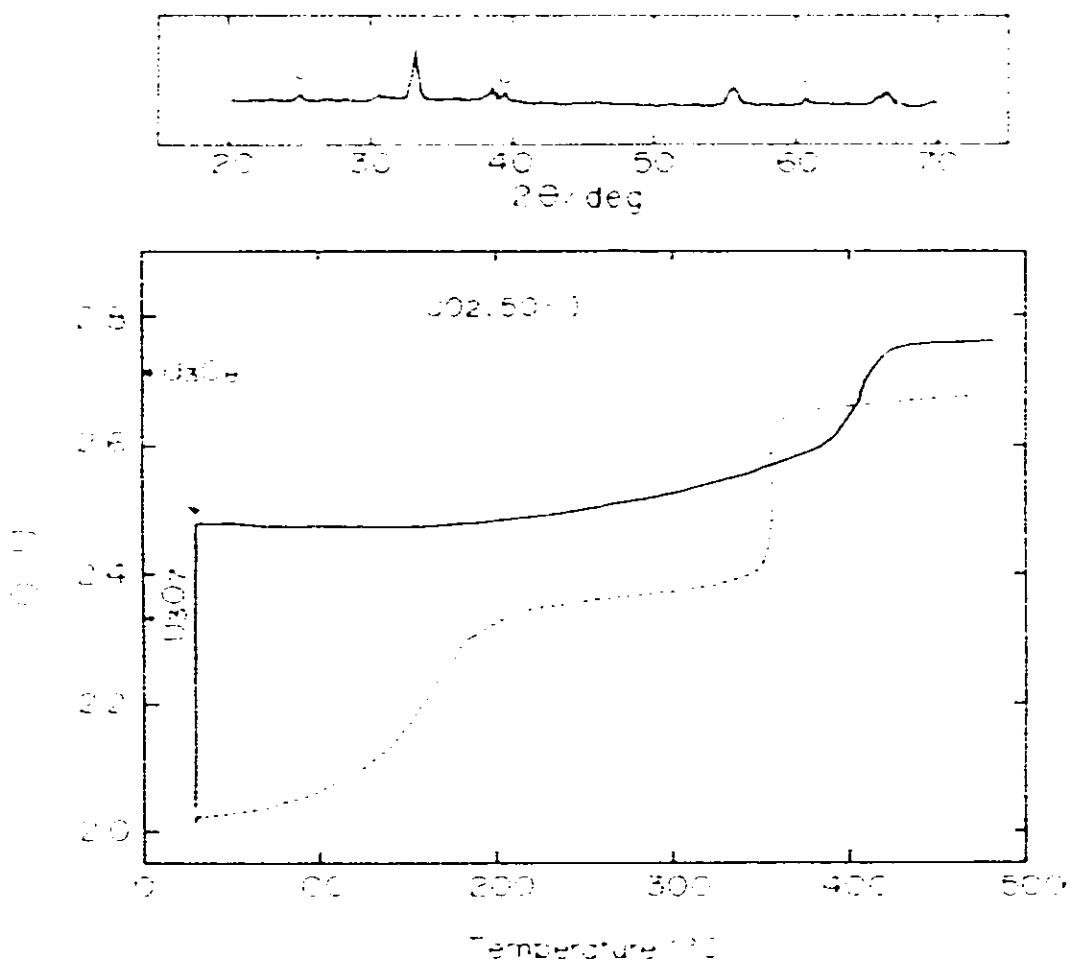

Fig. 10. TG curves of oxidation of UO_2(50-1) and X-ray diffraction pattern of the sample after oxygen uptake at room temperature (arrow on TG curve). ———, First oxidation; - - - - - -, second oxidation. TG: heating rate = 5°C min^{-1}; P_{O_2} = 150 mm Hg. X-Ray: = U_3O_8.

by the reduction of the U_3O_8 formed in the first oxidation. Table 3 shows the DSC peak temperatures. It is generally accepted that the oxidation of UO_2 proceeds through two consecutive steps from UO_2 to U_3O_7 (Step I) and from U_3O_7 to U_3O_8 (Step II) so that TG and DTA give curves with two plateaus and two exothermic peaks, respectively. As seen in Figs. 7—10, however, the shape of the TG and DSC curves becomes more complex depending on the preparation conditions of the samples. It is found from TG curves that (1) all UO_2 samples show oxygen uptake even at room temperature (vertical increment of O/U), (2) with an increase in temperature, the oxidation proceeds and Step I goes to completion at 250—350°C where the curve shows the plateau, (3) at higher temperatures after the plateau

TABLE 3

DSC peak temperature of the oxidation of UO_2 sample

Sample	First step, T_I (°C)	Second step, T_{II} (°C)
UO_2 (C)	221	363
UO_2 (50-8)	183	378
UO_2 (50-9)	192	T_{II_A} = 378, T_{II_B} = 408
UO_2 (52-4)	188	374
UO_2 (62-0)	194	T_{II_A} = 364, T_{II_B} = 385
UO_2 (45-5)	210	393
UO_2 (50-1)		

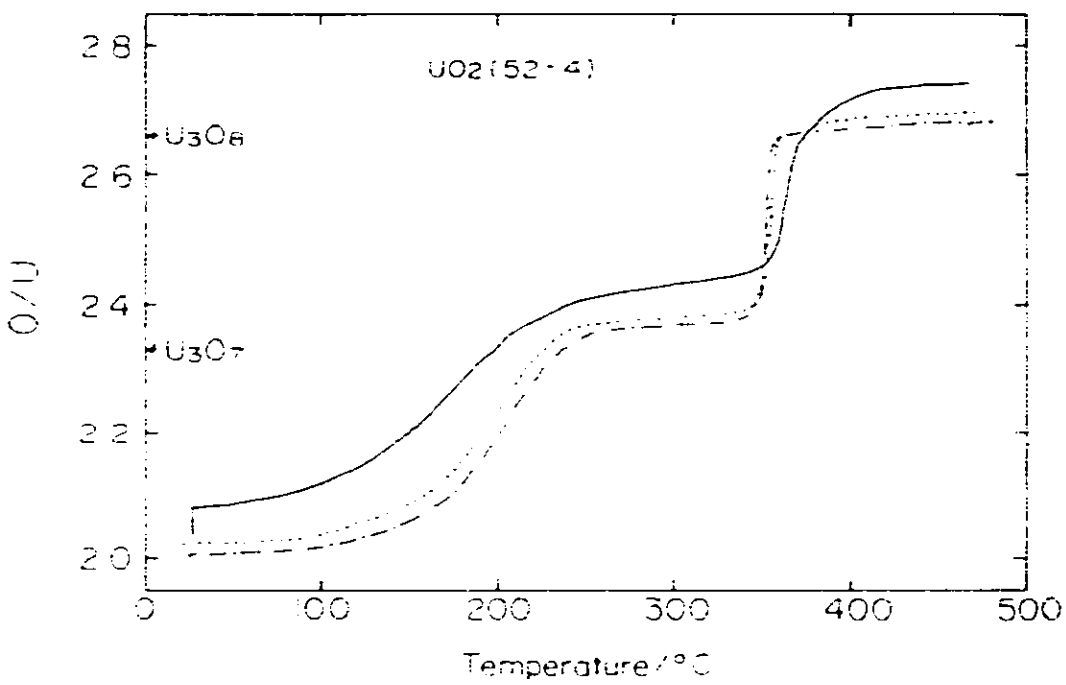

Fig. 11. Effect of repetition of oxidation on the TG result for UO_2(52-4). ———, First oxidation; - - - - - -, second oxidation; · — · — ·, third oxidation; heating rate = 5°C min^{-1}; P_{O_2} = 150 mm Hg. The reduction of oxidation product was carried out at $P_{H_2} + P_{N_2}$ = 100 + 50 mm Hg and 5°C min^{-1} up to 800°C.

period, Step II proceeds, and (4) in the cases of UO_2(50-9) and (62-0), Step II is subdivided into two stages (Step II_A and II_B). The increments of O/U corresponding to oxygen uptake at room temperature measured from TG curves are as follows; Δ(O/U) = 0.010 for UO_2(C), 0.038 for (50-8), 0.011 for (50-9), 0.042 for (52-4), 0.035 for (62-0), 0.025 for (45-5) and 0.445 for (50-1). It appears that the value of Δ(O/U) depends on the preparation conditions of the UO_3. High preparative temperatures and long preparative times may result in a small Δ(O/U). UO_2(50-1) derived from ADU has an extraordinarily large Δ(O/U). The X-ray diffraction pattern in Fig. 10 was obtained for UO_2(50-1) after the oxygen uptake at room temperature (arrow on the TG curve). The weak diffraction lines at 2θ = 25.0, 39.5 and 60.5° indicate the partial oxidation of UO_2(50-1) to U_3O_8 even at room temperature. The re-oxidation (dotted curve) shows the decrease in oxygen uptake from Δ(O/U) = 0.445 to 0.009. A similar decrease in the oxygen uptake was observed for other UO_2 samples by the repetition of the oxidation—reduction cycle, as shown in Figs. 11 and 12.

After oxygen uptake at room temperature, Step I proceeds with an increase in temperature. As found from Figs. 7—10 and Table 3, the prepared UO_2 samples show different oxidation behavior from UO_2(C); the TG curve and DSC peak (T_I = 183—210°C) of Step I for the prepared UO_2 are located in a lower temperature range compared with UO_2(C) (T_I = 221°C), and the O/U value on the plateau near 300°C is about 2.42 whereas for UO_2(C), O/U = 2.36. The value of 2.42 shows the formation of U_3O_{7+x} [6]. As seen in Fig. 10, UO_2(50-1) shows the large oxygen uptake at room temperature and Step I cannot be recognized in the first oxidation run. The re-oxidation develops Step I on the TG curve though the oxygen uptake at room temperature decreases. As observed in Figs. 11 and 12, the repetition of oxidation results in a shift in the TG curves towards a higher temperature range and a decrease in O/U from 2.42 to 2.36 near 300°C. These changes

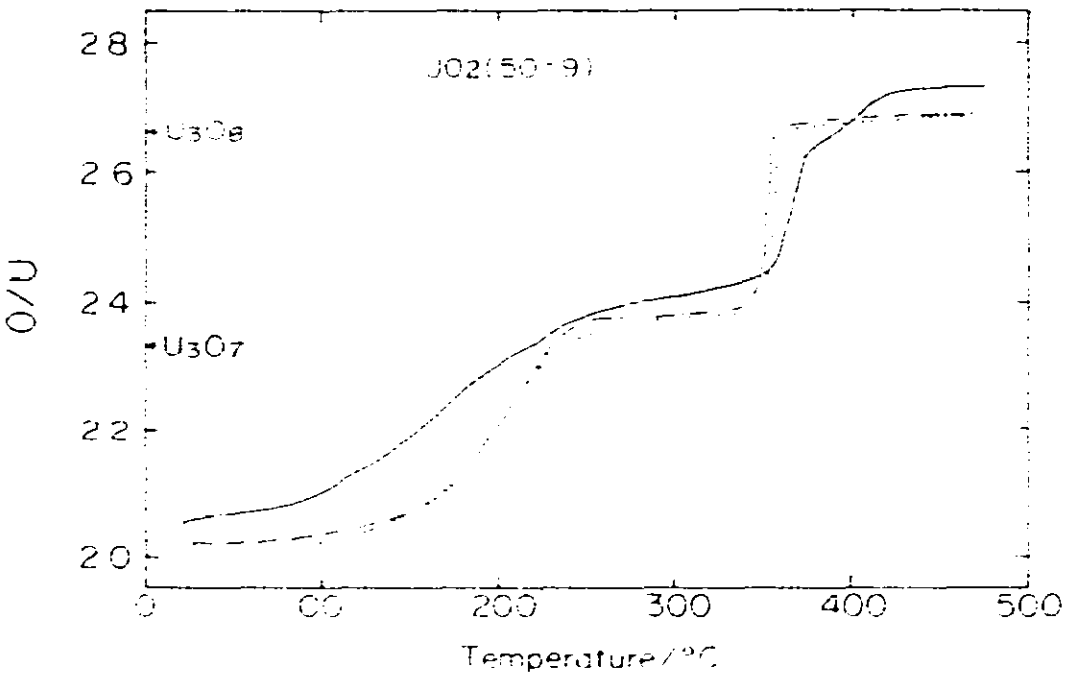

Fig. 12. Effect of repetition of oxidation on the TG result for UO_2(50-9).

indicate that the oxidation behavior of UO_2 prepared from UO_3 approaches that of UO_2(C) by the repetition of the oxidation—reduction ($UO_2 \leftrightarrows U_3O_8$) and suggest that U_3O_8 is the starting material for UO_2(C). Figure 13 shows the X-ray patterns of UO_2(50-8) samples obtained at various temperatures in the course of the oxidation. The cubic structure of β-UO_2 is kept up to 260°C during the oxidation though the diffraction lines are slightly shifted to higher 2θ with increasing temperature. This may mean that the oxygen is accommodated in the interstitial sites of the cubic lattice. The

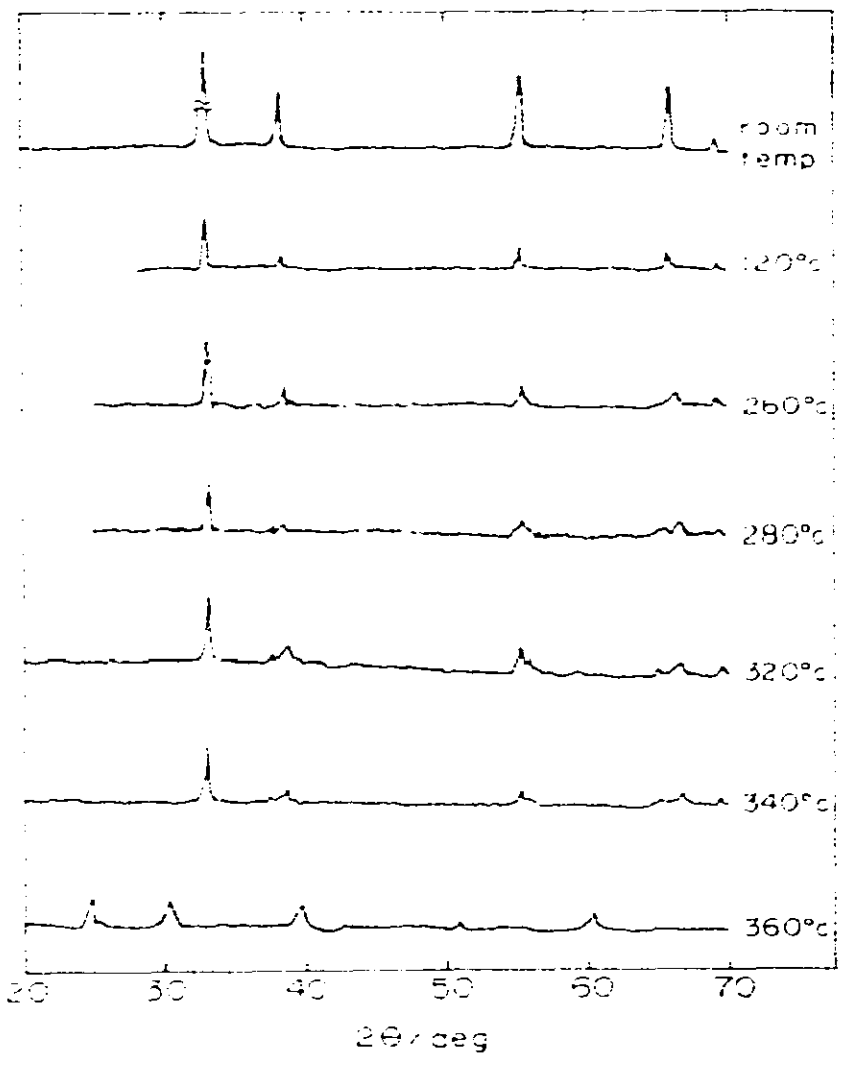

Fig. 13. X-Ray diffraction patterns of UO_2(50-8) samples taken out in the course of oxidation at various temperatures.

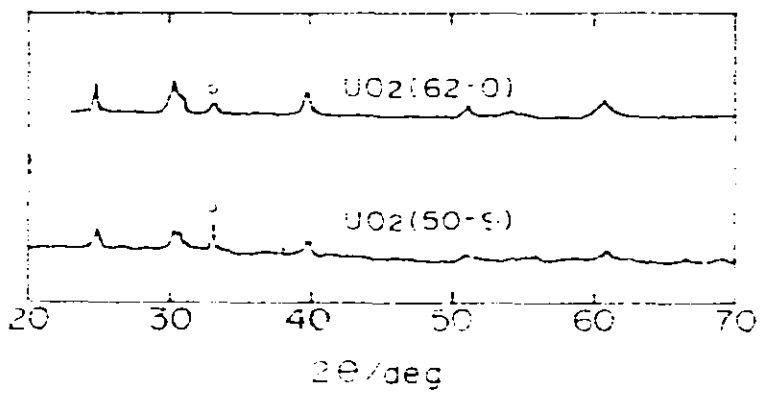

Fig. 14. X-Ray diffraction patterns of UO_2 samples taken out at the temperature between Step II_A and II_B shown by the arrow on the DSC curves in Figs. 8 and 9. Diffraction line of U_3O_7 is indicated by circle.

splitting of the lines at $2\theta = 38.5$ and 66.4° shows the formation of tetragonal U_3O_7 at 280°C. The formation of U_3O_8 is observed at 360°C. As found in Figs. 7—10, O/U values for 260—280°C are 2.35—2.36 for UO_2(C) and 2.40—2.42 for the prepared UO_2. Furthermore, Table 2 and Fig. 5 show that UO_2(C) has the large crystallite size and the sharp X-ray diffraction lines. It is considered that UO_2(C) is less defective and has a small interstitial volume for oxygen accommodation, which leads to the high temperature oxidation of Step I compared with the prepared UO_2. The repetition of the oxidation—reduction of the prepared UO_2 is thought to cause the decrease in the interstitial volume.

Step II proceeds in a rather narrow temperature range above 350°C and a sharp exothermic DSC peak is obtained in contrast to the broad peak of Step I. As found from the TG and DSC curves in Figs. 8 and 9, Step II of UO_2 (50-9) and (62-0) splits into two sub-steps (Step II_A and II_B). The DSC curve of UO_2(52-4) shows a small shoulder at 395°C which may also be due to Step II_B. Figure 14 shows the results of the X-ray diffraction of samples removed at the temperatures shown with an arrow between the two DSC peaks corresponding to Step II_A and II_B in Fig. 8 (395°C) and Fig. 9 (372°C). Figure 14 indicates some remaining U_3O_7 (∘) in addition to the formation of U_3O_8. This fact leads to an assumption that in the course of Step I two kinds of U_3O_7 are formed and they have different reactivities with respect to oxidation. Two modifications of U_3O_7 (α and β) have been reported [7], but the broad X-ray lines in Fig. 14 do not provide a clue as to the distinction between the α and β form. The formation of two U_3O_7 of different reactivities can be considered to be due to the preparation conditions of UO_3 from which UO_2 and U_3O_7 are successively formed. As shown in Table 1 and Fig. 2, UO_3(50-9) is a mixture of α-UO_3 and γ-UO_3, and UO_3-(62-0) is a mixture of α-UO_3 and U_3O_8. It is assumed that the oxidation temperature of UO_2 and U_3O_7 produced from α-UO_3 is different from that of the oxides produced from other forms of UO_3 and U_3O_8. It is observed in Table 3 that the DSC peak temperature (T_{II}) of UO_2(C) is 363°C which is the same as T_{II_A} for UO_2(62-0). Since UO_2(62-0) is formed from a mixture of U_2O_8 and α-UO_3 and the starting material of UO_2(C) was U_3O_8 as presumed previously, the peak at 363°C is considered to correspond to the oxidation of a sample formed from U_3O_8. Next, the peak temperature of T_{II} for UO_2(50-8) and

(52-4), and T_{II_A} for UO_2(50-9) are 378, 374 and 378°C, respectively. These UO_2 samples were all obtained from UO_3 samples containing γ-UO_3. Finally, T_{II_B} for UO_2(50-9) and (62-0), and T_{II} for UO_2 (45-5) are 408, 385 and 393°C, respectively. These higher T_{II} values may correspond to the oxidation of samples formed from α-UO_3 though they vary between 385 and 408°C. Figure 12 shows the TG curves for three successive repeat oxidations of UO_2(50-9). It is found that the repetition changes Step II from a two step oxidation in the first run (solid curve) to a one step oxidation in the second and third run (dotted curves), and the shape of the TG curves approachs that of UO_2(C). UO_2(C) shows a plateau above 380°C and forms the stoichiometric U_3O_8 (O/U = 2.67) as seen in Fig. 7. On the other hand, TG curves of the prepared UO_2 (Figs. 7—10) show higher O/U values between 2.72 and 2.75 which indicate the formation of U_3O_{8+x}. Furthermore, T_{II} for UO_2(C) is the lowest (363°C). This suggests that almost stoichiometric U_3O_7 formed from UO_2(C) is less stable than the U_3O_{7+x} formed from UO_3 samples. The oxidation of Step II has been explained by the rate of nucleation and growth of U_3O_8 in the U_3O_7 phase, thus the excess oxygen in U_3O_{7+x} is considered to hinder the rearrangement of oxygen ions to form the nuclei so that the prepared UO_2 shows high T_{II} values.

Figure 15 shows the Kissinger's plots for the estimation of the activation energy, E_I for Step I and E_{II} for Step II. The DSC peak of Step I was broad as seen in Figs. 7—9 and the peak temperature for UO_2(50-9) could not be measured where the heating rates were low. Therefore, the plots for E_I show some scatter. Figure 16 is the relation of the DSC peak temperature to E_I and E_{II}. It is found that the oxidation occurring at higher temperatures needs a high E value. The four repeat oxidations of UO_2(50-8) resulted in

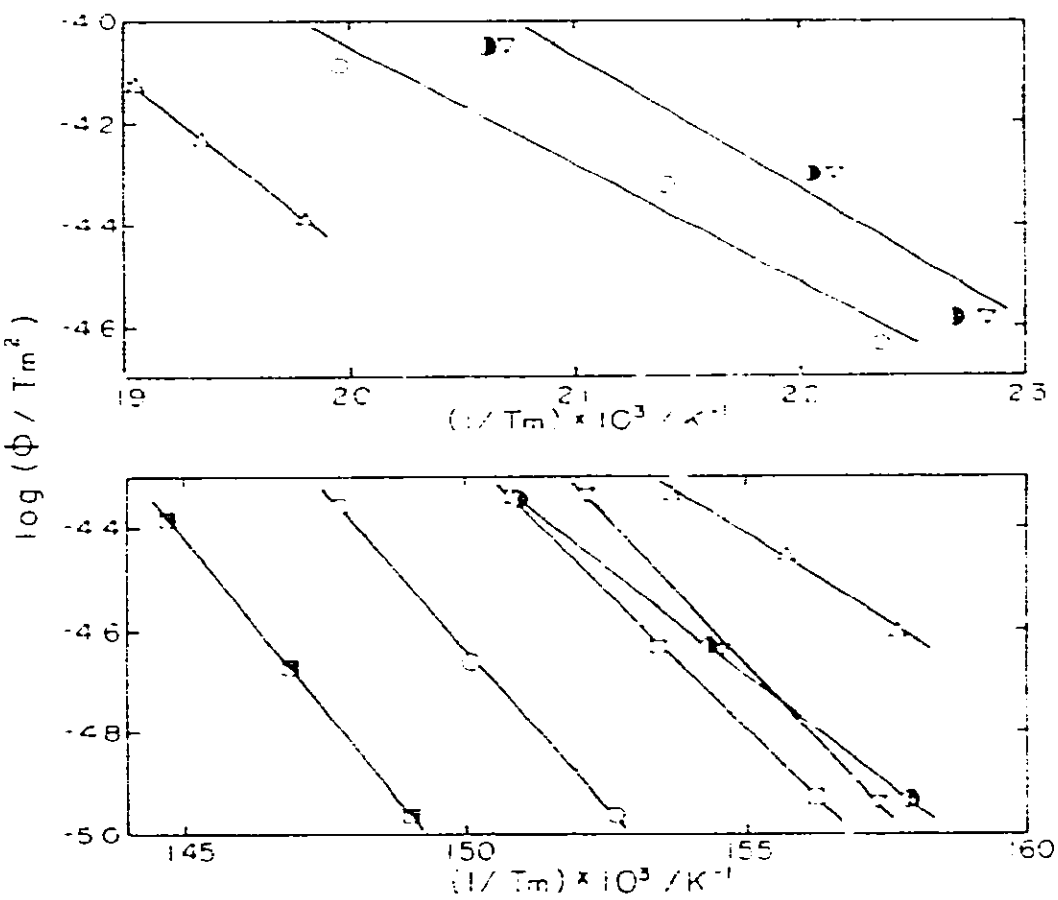

Fig. 15. Kissinger's plots of DSC results of oxidation of UO_2. △, UO_2(C); ○, UO_2(45-5); ▽, UO_2(50-8); ◑, UO_2(52-4); □, UO_2(50-9) Step II_A; ■, UO_2(50-9) Step II_B.

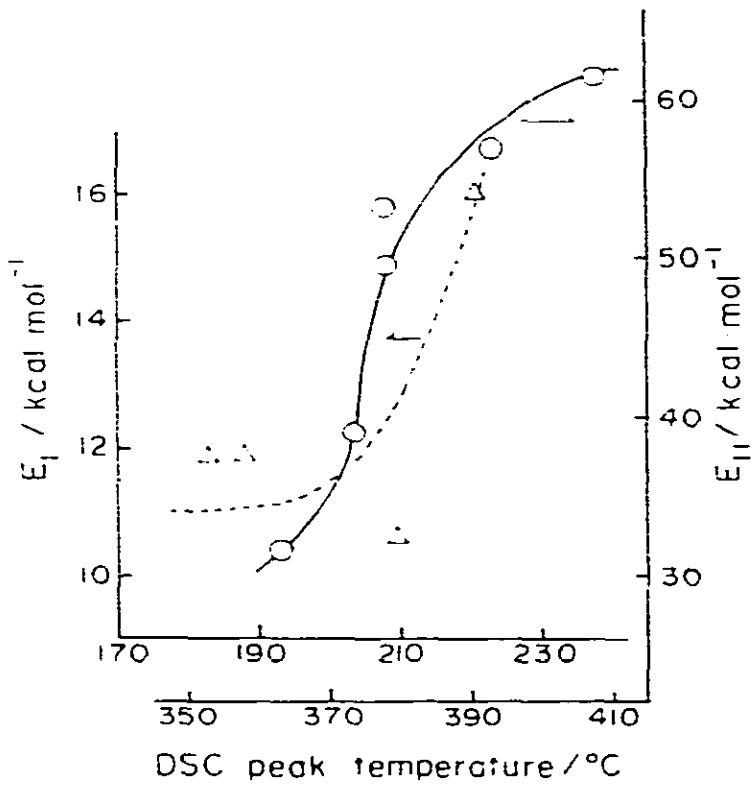

Fig. 16. Relation between activation energy and the DSC peak temperature of UO_2 oxidation. E_I is for Step I and E_{II} is for Step II.

$E_I = 12.8$ and $E_{II} = 33.3$ kcal mole^{-1} which are comparable with $E_I = 16.0$ and $E_{II} = 31.6$ kcal mole^{-1} for UO_2(C).

ACKNOWLEDGEMENTS

The authors would like to thank Mr. Z. Yamanaka for taking photographs of samples by SEM. This research has been partially supported by a Government Science Research Grant from the Ministry of Education, Japan.

REFERENCES

1 K.B. Alberman and J.S. Anderson, J. Chem. Soc., (1949) 303.
2 J.S. Anderson, L.E.J. Roberts and E.A. Harper, J. Chem. Soc., (1955) 3946.
3 J.R. Johnson, S.D. Fulkerson and A.J. Taylor, Ceram. Bull., 36 (1957) 112.
4 J.S. Anderson, R.B. Roof, Jr. and J. Belle, J. Chem. Phys., 27 (1957) 137.
5 P.E. Blackburn, J. Weissbart and E.A. Gulbransen, J. Phys. Chem., 62 (1958) 902.
6 R.E. DeMarco, H.A. Heller, R.C. Abbott and W. Burkhardt, Ceram. Bull., 38 (1959) 360.
7 H.R. Hoekstra, A. Santoro and S. Siegel, J. Inorg. Nucl. Chem., 18 (1961) 166.
8 D. Kolar, E.D. Lynch and J.H. Handwerk, J. Am. Ceram. Soc., 45 (1962) 141.
9 K.T. Scott and K.T. Harrison, J. Nucl. Mater., 8 (1963) 307.
10 T. Ishii, T. Furumai and G. Takeya, Kogyo Kagaku Zasshi, 70 (1967) 1952.
11 V.J. Tennery and T.G. Godfrey, J. Am. Ceram. Soc., 56 (1973) 129.
12 H. Ohashi, E. Noda and T. Morozumi, J. Nucl. Sci. Technol., 11 (1974) 445.
13 D.A. Vaughan, J.R. Bridge, A.G. Allison and C.M. Schwartz, Ind. Eng. Chem., 49 (1957) 1699.
14 E.H.P. Cordfunke and A.A. Van der Giessen, Proc. 5th Int. Symp. Reactivity Solids, Elsevier, Amsterdam, 1965, p. 456.
15 E.H.P. Cordfunke, The Chemistry of Uranium Including its Applications in Nuclear Technology, Elsevier, Amsterdam, 1967.

16 S. Shimada, R. Furuichi and T. Ishii, Bull. Chem. Soc. Jpn., 49 (1976) 1289.
17 T. Tsuchida, R. Furuichi and T. Ishii, Z. Anorg. Allg. Chem., 415 (1975) 175; 423 (1976) 180.
18 M. Shimokawabe, R. Furuichi and T. Ishii, Thermochim. Acta, 20 (1977) 347; 21 (1977) 273.
19 R. Furuichi, M. Shimokawabe and T. Ishii, Proc. 5th Int. Conf. Therm. Anal., Kagaku Gijutshu—Sha, Tokyo, 1977, p. 512.
20 T. Ishii, R. Furuichi and Y. Hara, J. Therm. Anal., 11 (1977) 71.
21 M.C. Ball, C.R.G. Birkett, D.S. Brown and M.J. Jaycook, J. Inorg. Nucl. Chem., 36 (1974) 1527.
22 W. Biltz and H. Muller, Z. Anorg. Allg. Chem., 163 (1927) 257.
23 Y. Saito, Nestusokutei, 3 (1976) 68.
24 R.M. Dell and V.J. Wheeler, Trans. Faraday Soc., 58 (1962) 1950.
25 R.E. DeMarco and M.G. Mendel, J. Phys. Chem., 64 (1960) 132.
26 A.H. LePage and A.G. Frane, J. Inorg. Nucl. Chem., 36 (1974) 87.